ACS Catalysis

pubs.acs.org/acscatalysis
Research Article

β-Scission of Secondary Alcohols via Photosensitization: Synthetic Utilization and Mechanistic Insights

Yeersen Patehebieke, Rima Charaf, Hogan P. Bryce-Rogers, Ke Ye, Mårten Ahlquist, Leif Hammarström, and Carl-Johan Wallentin*

Cite This: ACS Catal. 2024, 14, 585−593
Read Online

ACCESS | Metrics & More | Article Recommendations | Supporting Information

ABSTRACT: An efficient metal-free photocatalytic method for the alkylation of alkenes using accessible aliphatic alcohols as redox auxiliaries is presented. C-centered radicals can be generated under mild conditions and subsequently employed in a $C(sp^3)-C(sp^3)$ bond-forming process, which overall provides a C1 tethering strategy of nucleophiles and electrophiles. The optimized conditions accommodate various electron-deficient alkenes and secondary/tertiary alcohols, with applications in late-stage functionalization of natural products and pharmaceutically relevant compounds. Mechanistic investigations revealed a complex mechanistic manifold, including non-PCET fragmentation and concerted/stepwise PCET. Even though the previously thought PCET type mechanism is compatible with our observations, the non-PCET mechanism most probably constitutes a main pathway.

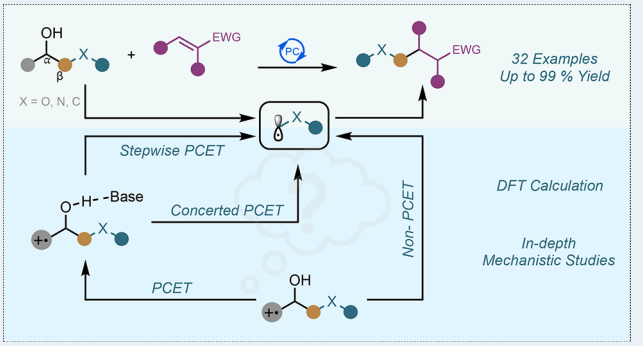

KEYWORDS: *PCET, C1 tethering, Giese type reaction, alkoxy radical, photocatalysis*

INTRODUCTION

Alkoxy radicals are well-known and highly reactive transient species that provide valuable synthetic opportunities.[1] However, despite the vast array of synthetic possibilities, there are only a limited number of reliable and benign methods for creating and employing alkoxy radicals in the production of molecular intricacy.[2]

Hydroxyl groups, which are an immediate source of oxygen-centered radicals, are widely present in natural products,[3] pharmaceuticals,[4] and chemical feedstock compounds,[5] and can conveniently be derived from a multitude of functionalities like alkenes, ketones, aldehydes, etc.[6] Therefore, the direct generation of oxygen centered radicals from free alcohols constitutes a straightforward and economical pathway to access a plethora of such valuable high energy intermediates. However, due to the high bond dissociation energy (BDE ∼ 105 kcal mol^{-1})[2,7] of the alcohol O−H bond, the direct formation of an alkoxy radical from free alcohols is challenging. Consequently, traditional methods predominantly rely upon prefunctionalized radical precursors such as nitrite esters,[8] hypohalites,[9] peroxides,[10] sulfenates,[11] *N*-alkoxyphthalimides,[12] and *N*-alkoxypyridinium salts[13] to achieve weak O−X bonds able to more efficiently undergo thermal/photo/radical induced homolysis to generate alkoxy radicals (Figure 1A).[1a,2] Employing such prefunctionalized alcohol-auxiliary precursors has the drawback of tedious synthetic prefunctionalization and purification,[14] poor stability,[15] toxicity,[16] and/or narrow functional group tolerance, which hampers their synthetic potential.

Over the past decade, the growth of transition-metal and photoredox catalysis has resulted in new protocols that can generate alkoxy radicals directly from free alcohols without prefunctionalization (Figure 1A).[1a,1,2] Moreover, many of these approaches require the use of stoichiometric amounts of strong oxidants (such as $K_2S_2O_8$, selectfluor, or hypervalent iodine reagents),[17] which consequently present limitations in terms of functional group tolerance and thus their applicability in more challenging synthetic endeavors.

Photoinduced proton-coupled electron transfer (PCET) and ligand-to-metal charge transfer (LMCT) methods, pioneered by Zuo and Knowles, have enabled direct access to oxygen-centered radicals from unfunctionalized alcohols in a redox-neutral manner (Figure 1A). In 2016, Zuo's group reported a $CeCl_3$-catalyzed photocatalytic LMCT-mediated amination of cycloalkanols.[18] In the same year, Knowles and co-workers developed the first catalytic ring-opening of cyclic alcohols enabled by PCET.[19] Since then, these elegant strategies have

Received: October 27, 2023
Revised: December 12, 2023
Accepted: December 12, 2023
Published: December 26, 2023

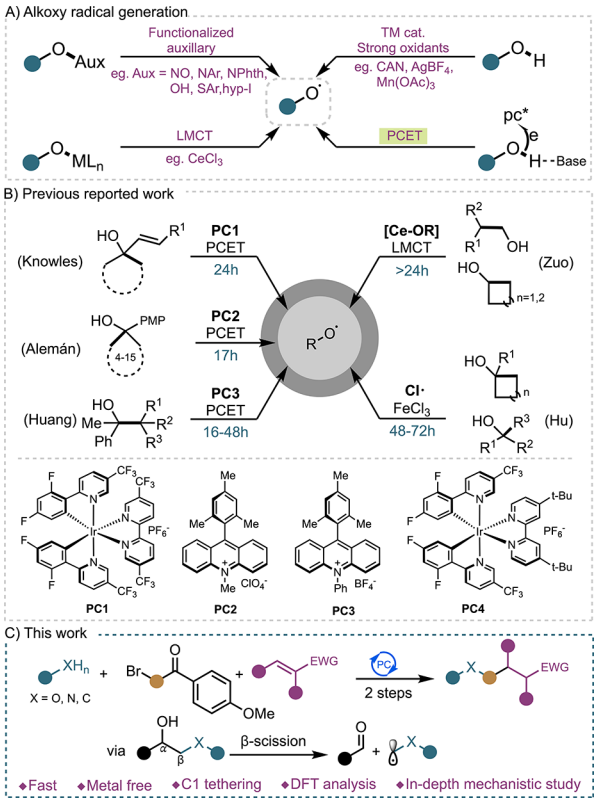

Figure 1. (A) Alkoxy radical generation strategies. (B) Previously reported photocatalytic alkylation of alkenes by free alcohols. (C) This work: visible light induced one carbon tethering technique for the alkylation of alkenes by free alcohols.

inspired the emergence of a renaissance in the field of direct alkoxy radical generation from free alcohols.[20] To date a platform for alkoxy radical-mediated redox-neutral transformations under mild conditions has in part been established.[21] However, most of the reported photocatalytic PCET and LMCT-based methods have been restricted to cycloalkanols and/or employed precious metal(photo)-catalysts.[1,2] Considering the significance of alkoxy radicals in organic synthesis,[1] it is highly desirable to develop more sustainable and general catalytic protocols for the generation and the subsequent application of alkoxy radicals directly from free acyclic alcohols without using metal catalysts.

Common synthetic utilization of alkoxy radicals involves β-scission followed by C−C bond formation with the so-formed C-centered radical. This is often referred to as a deconstructive approach toward the functionalization of alcohols. Only a few examples of photocatalytic alkylation of olefins by deconstruction of aliphatic alcohols have been reported (Figure 1B). Notably, most of these methods are dependent on specific types of alcohol and olefin substrates. For example, the Iridium photocatalyst (PC1) was used by the Knowles group in inter and intramolecular transformations only applicable with 1-vinyl alcohols (Figure 1B).[20b,22] The Ce-catalyzed procedures developed by Zuo and co-workers require strained cyclic alcohols or primary alcohols that produce stable alkyl radicals (Figure 1B).[20j,k] Similarly, specific phenyl-substituted tertiary or cyclic alcohols where needed in acridinium catalyzed (PC2 & PC3) Giese type additions recently developed by the Aleman group and the Huang group (Figure 1B).[23]

Recently, Hu's group realized photoinduced iron-catalyzed deconstructive alkylation of electron-deficient alkenes via chlorine radical mediated C−C single bond fragmentation of aliphatic alcohols (Figure 1B).[21k] So far, this strategy has tolerated a broader range of alcohols and alkenes. However, there is no general and quick method available to achieve the alkylation of alkenes by radicals directly generated from alcohols through C−C bond cleavage.

Herein, we present a metal-free photocatalytic method for the alkylation of alkenes utilizing aliphatic secondary alcohols as redox auxiliaries. The initial design strategy involved an envisioned indirect PCET mode of activation of this radical precursor in line with the approach perused by Alemán, Huang, and others. This would provide an alkoxy radical intermediate via β-scission and thus a possibility for deconstructive C−C bond-forming transformations. By employing the installment of the auxiliary as a C1 building block in an overall tethering strategy of nucleophiles and electrophiles (Figure 1C), a completely new way to connect such typical reaction partners could be realized.

RESULTS AND DISCUSSION

The methoxy-substituted substrate **1a** was chosen as a point of departure in the study since the electron-rich aromatic entity would allow for an efficient reductive quenching of the photocatalyst excited state. The so-formed nucleophilic radical would constitute a potent reactant in Giese-type additions, and consequently, the vinylic sulfone **2j** was selected as the electrophilic counterpart. (Table 1). After an extensive

Table 1. Optimization of Reaction Conditions[a]

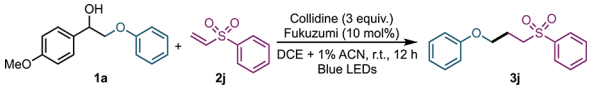

entry	deviation from standard conditions	yield (%)[b]
1	no deviation	53
2	24 h	59
3	48 h	64
4	$[Ir(dF(CF_3)ppy_2dtbbpy)]PF_6$	44
5	5% acetonitrile	63
6	$(n\text{-}Bu)_4P^+$ $(PhO)_2(O)PO^-$	59
7	no photocatalyst	n.d.
8	no light	n.d.
9	no base	n.d.

[a]Reaction conditions: **1a** (0.3 mmol), **2j** (0.1 mmol), Fukuzumi catalyst (10 mol %), 2,4,6-collidine (3 equiv), DCE + CH_3CN (3 mL), blue LED irradiation for 12 h at room temperature. [b]Yields were determined by the ^1H NMR analysis of crude reaction mixtures using ethylene carbonate as an internal standard.

screening of photocatalysts, solvents, bases, and stoichiometry of the reagents,[24] optimal reaction conditions were established. The targeted addition product **3j** was obtained, with a 63% yield in 12 h, by using the Fukuzumi catalyst (PC2), 2,4,6-collidine as a base, and a solvent mixture of 1,2-dichloroethane (DCE) + 5% acetonitrile at room temperature (Table 1, entry 5). Although prolonged reaction time showed increasing trends in yield (Table 1, entries 2 and 3), the increase was not significant. Therefore, a 12 h reaction time was selected since considered the most efficient overall. Comparable results were obtained with the catalyst $[Ir(dF(CF_3)ppy_2dtbbpy)]PF_6$ (PC4) (Table 1, entry 4), while all the other evaluated

https://doi.org/10.1021/acscatal.3c05150
ACS Catal. 2024, 14, 585−593

photocatalysts performed worse (other photocatalysts evaluated are presented in the optimization of reaction conditions section in the ESI). Therefore, the Fukuzumi catalyst was selected as the optimal and most readily available catalyst.

Interestingly, introducing acetonitrile as a cosolvent improved the reaction efficiency which was reflected in an increased alcohol consumption: β-scission ratio. With 5% acetonitrile the highest product yield and cleanest transformation was observed (Table 1, entry 5 and for results of other ratios of additive see optimization of reaction conditions section in the ESI).

Among all assessed bases, only tetrabutylphosphonium diphenyl phosphate base presented decent comparable results with collidine (Table 1, entry 6). However, due to the hydroscopic nature and the necessity to synthesize this base, collidine was selected as the ideal base (for results of other tested bases, see optimization of reaction conditions section in the ESI).

Finally, control experiments confirmed that no products could be detected when either photocatalyst, base, or blue light irradiation were excluded from the system (Table 1, entries 7–9).

With the optimized conditions in hand, we turned our attention to exploring the scope of the protocol with various Michael acceptors. Taken together, the developed reaction conditions showed to be applicable to a rather wide array of electron-deficient alkenes (Table 2). The best yielding substrates, β-alkyl and β-aryl substituted methylene-malonates, provided the targeted **3a** and **3b** in 99 and 80% yield, respectively.

Acrylates and fumarates, e.g., butyl methacrylate and dimethyl fumarate, are also suitable substrates, readily affording the corresponding alkylated products in >70% yields (**3c** and **3d**). Alkylation of other β-substituted electron-deficient olefins, such as benzalmalononitrile, 1,2-dibenzoylethene, benzylideneacetone, and 3-methyl-3-penten-2-one, also proceeded smoothly to give the desired products **3e**, **3f**, **3g**, and **3h** in moderate to excellent yields (37–84%). Ketone, sulfone, nitrile, and amide-substituted olefins (**3i**, **3j**, **3k**, **3l**) were also susceptible to the conditions, although giving the alkylated products in somewhat lower yields (20–62%).

It is worth mentioning that with compounds prone to polymerization, there is a significant drop in the yield, particularly for those with no sterically demanding group in the α-position. Examples of these are **3g** and **3j–l**.

This tendency has previously been reported for photocatalyzed Giese type addition reactions.[25] However, dimethyl fumarate, which is unsubstituted at the alpha-position, still generated significantly high yields, which in this case can be explained by the electronic effect imposed by this dually activated compound. It is simply constituted in such a way that the activation energy for the addition reaction is more favored than polymerization.

After satisfactory results were obtained from olefin coupling partners, the investigation shifted to the substrate scope of alcohols.

Both secondary alcohols (**1**) and tertiary alcohols (**1o**) were evaluated. Gratefully, all of the examined alcohols, except (**3q**), showed sufficient reactivities, resulting in moderate to excellent isolated yields of the desired alkylated products (Table 3). Alkyls with and without heteroatoms, cyclic alkyls, linear alkyls, benzyl and heterocycles, where all compatible with the conditions.

In more detail, neutral (**3a**, **3f**), weak electron-donating (**3m**, **3o**), and electron-withdrawing group (**3n**, **3p**) substituted phenolic derivatives showed satisfactory reactivity, resulting in good to almost quantitative yields of the desired products (77–99%). However, for the three substrates **3f**, **3n**, and **3o**, purification difficulties were encountered, which reduced the isolated yields somewhat. Hence, the coupling partner 1,2-dibenzoylethene was changed to diethyl 2-ethylidenemalonate for the rest of the investigation. Surprisingly, for electron-rich guaiacol, **3q**, and 2-naphthol derivative, **3r**, a palpable decrease in yield was observed. When employing **3q** as a substrate poor conversion to the aldehyde side product was observed, implying that the electron-rich moiety stabilizes the intermediate radical cation to such an extent that the β-scission based fragmentation yielding the C-centered radical is not accessible (vide infra).

Furthermore, we also wanted to explore if α-aza- and α-thio C-centered radicals, generated from the corresponding congeners of **1a**, would display analogues reactivity as compared to that of the α-oxo C-centered radical. Indeed, satisfactory results were obtained with aniline and amine-derived alcohols, which presented good reactivity giving products in moderate to good yields (**3aa–3ad**, 21–73%). It should be mentioned that an attempt at using a secondary aniline derivative was also made; however, no fragmentation of the starting materials or any generation of product was observed. Subjecting the thio derivative of **1a** to identical reaction conditions did promote β-scission and thus the generation of the α-thio C-centered radical, however, no product formation was observed.

Finally, to illustrate the potential of the developed method in the late-stage functionalization of natural products or pharmaceutically relevant compounds, we subjected ezetimibe (a drug used to treat high blood cholesterol levels) and an

Table 2. Scope of Olefin Substrates[a,b]

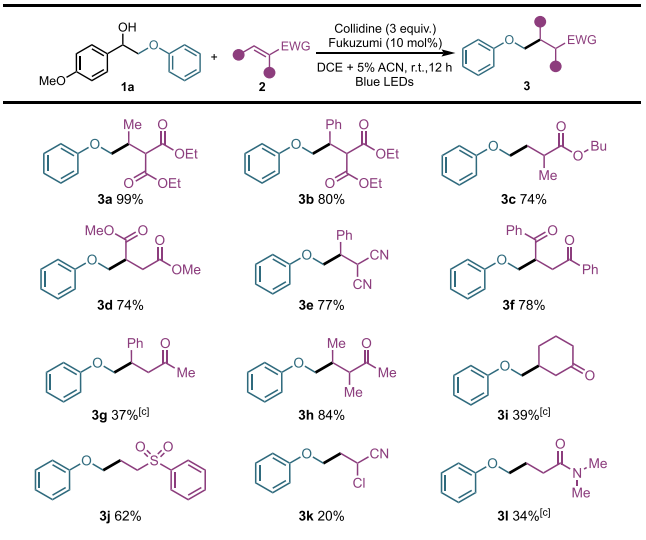

[a]Reaction conditions: alcohol substrate **1a** (0.3 mmol), alkene substrate **2** (0.1 mmol), Fukuzumi catalyst (10 mol %), 2,4,6-collidine (3 equiv), DCE + 5% CH_3CN (3 mL), blue LED irradiation for 12 h at room temperature. [b]Reported yields are for isolated and purified material and are the average of two experiments. [c]^{1}H NMR yield are given using ethylene carbonate as the internal standard.

https://doi.org/10.1021/acscatal.3c05150
ACS Catal. 2024, 14, 585–593

Table 3. Scope of Alcohol Substrates[a,b]

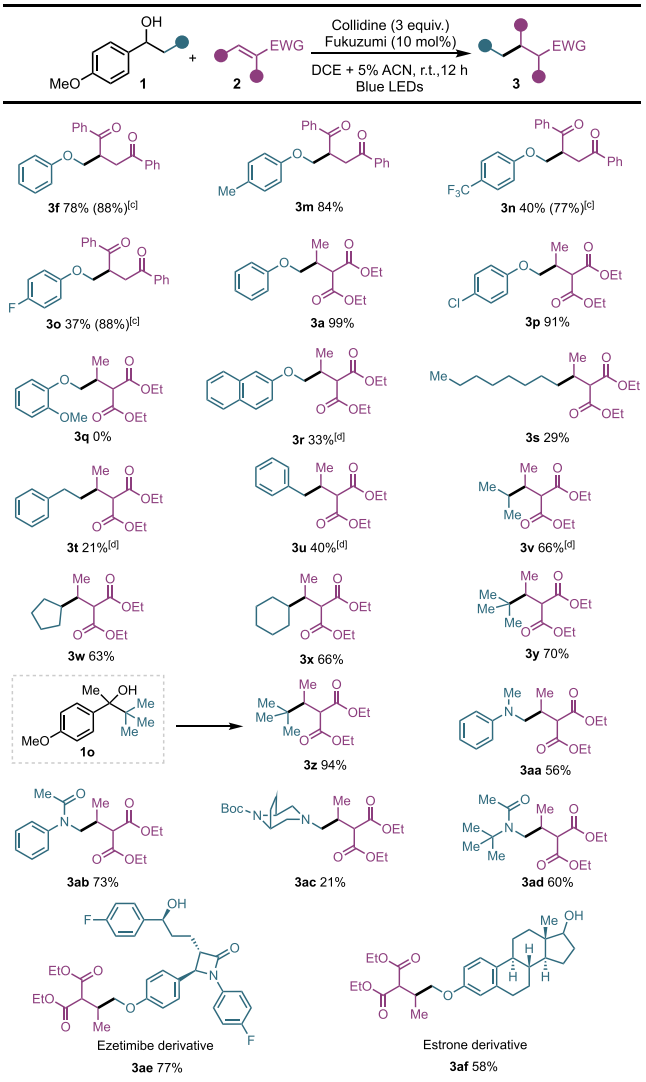

[a]Reaction conditions: alcohol substrate **1** (0.3 mmol), alkene substrate **2** (0.1 mmol), Fukuzumi catalyst (10 mol %), 2,4,6-collidine (3 equiv), DCE + 5% CH_3CN (3 mL), blue LED irradiation for 12 h at room temperature. [b]Reported yields are for isolated and purified material and are the average of two experiments. [c]Complication in the purification of compound with side products decreased the isolated yield, inside the bracket is the ^{1}H NMR yield. [d]^{1}H NMR yield are given using ethylene carbonate as the internal standard.

estrone derivative (**3ae**, **3af**) to the optimized conditions involving α-oxo C-centered radicals. Excitingly, both derivatives of this late-stage functionalization were obtained in good yields, **3ae** in 77% and **3af** in 58% yield.

Mechanistic Investigations. Based on the previous published reports, we hypothesized a plausible PCET-based mechanism for this photocatalytic alkylation reaction of alkenes by free alcohols, which is illustrated in Figure 2. Upon irradiation with visible light, the ground state of the Fukuzumi catalyst, PC (**a**), is excited to a highly oxidizing singlet excited state PC* (**b**). Reductive quenching of this state by the substrate furnishes the corresponding arene radical cation (**e**) along with the reduced form of the photocatalyst PC

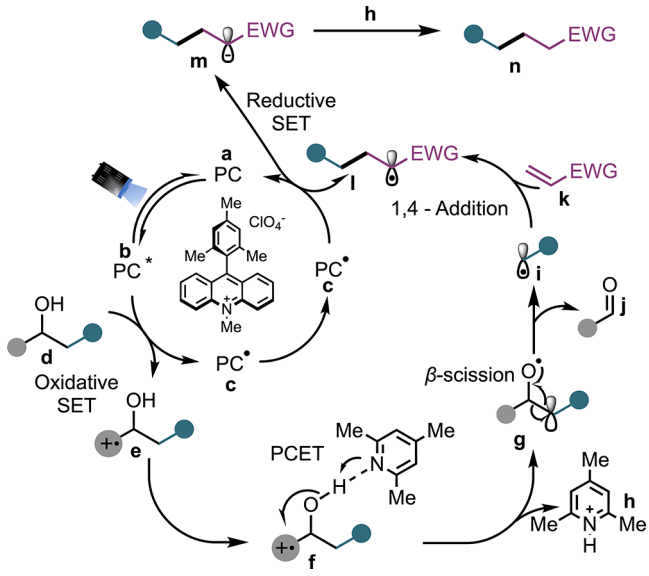

Figure 2. Proposed mechanism based on the literature.

(**c**). This is supported by the studies performed by Steenken and Baciocchi in the early 2000s,[26] as well as the later works published by Knowles[19,20b] and Rueping.[21a,d] It is essential that the aromatic entity employed as the active reductive quencher for this specific catalyst is an anisole derivative since the redox potential needs to be low enough to provide a thermodynamic driving force for the quenching process.[27] The now oxidized substrate (**e**) is believed to undergo a PCET (**f**) to generate a key alkoxyl radical species (**g**),[19,20b,21a] which subsequently cleaves into an alkyl radical (**i**) and a side product aldehyde (**j**) through β-fragmentation.[17f,20j] Then, the in situ capture of this formed alkyl radical (**i**) by an olefin (**k**) produces a radical addition product (**l**). Finally, the radical addition product is reduced by the reduced PC (**c**) and subsequent protonation by protonated base (**h**) to yield the desired alkylation product (**n**) and regenerate the photocatalyst and base to close the catalytic cycle.

Upon scrutinizing possible mechanistic pathways, it became evident that the oxidation of the substrate could evolve via five potential routes to give radical **IVa** (Figure 3A). The PCET-based stepwise fragmentation described above, which currently is believed to be the operating mechanism, does not necessarily constitute the main operating mechanism. It might actually not be operating at all.

To gain a better understanding of the reaction mechanism, we thus performed a series of experimental and computational studies. The energy profiles of the key mechanisms were mapped using DFT calculations and these are, together with schematic representations of relevant transition states, displayed in Figure 3A, B (for computational details and depicted spin density maps of relevant species, see DFT calculation section in the ESI).

The DFT calculations revealed that there are three main pathways for the generation of the C-centered radical: (A) a base-independent non-PCET fragmentation, (B) a concerted PCET not involving an alkoxy radical intermediate, and (C) a stepwise PCET progressing via formation of an alkoxy radical. The latter pathway is in accordance with the current view of the operating mechanism.

From the energy profiles (Figure 3B) we can observe that the concerted PCET (pathway B) is associated with a lower

https://doi.org/10.1021/acscatal.3c05150
ACS Catal. 2024, 14, 585−593

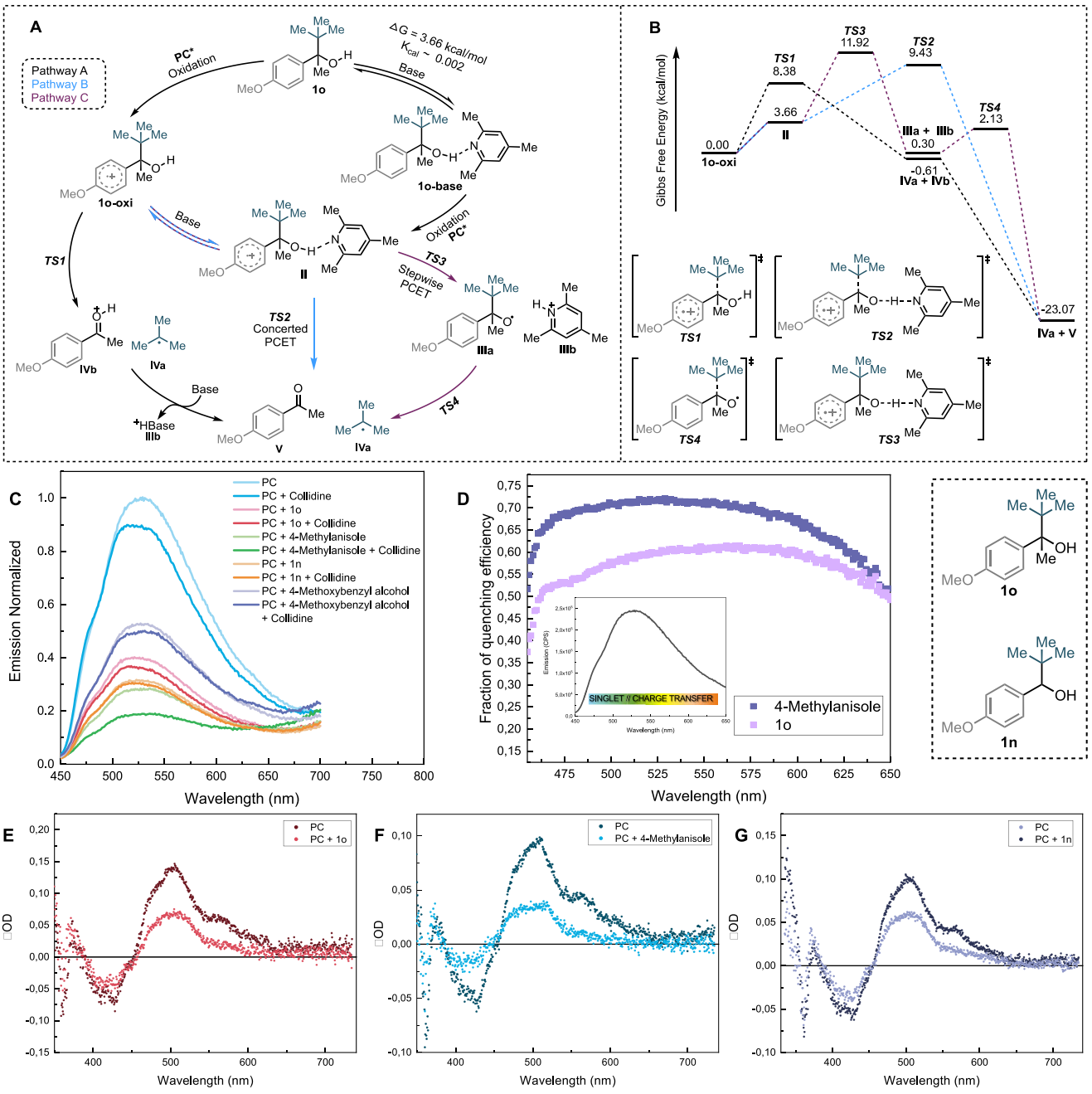

Figure 3. (A) Possible pathways suggested by DFT calculation. (B) DFT calculation energy profile and structures of the transition states. (C) Quenching of emission with various substrates (40 mM). Addition of collidine (10 mM) does not enhance the quenching (only an additive effect and not cooperative). (D) Fraction of quenching efficiency of Fukuzumi catalyst emission with two different substrates (40 mM), calculated as $1 - I_{quencher}/I_0$, where $I_{quencher}$ and I_0 are the emission intensities in presence and absence of quencher, respectively. The inset shows the different areas of contribution of the acridinium and charge transfer states to the fluorescence spectrum of the Fukuzumi catalyst. (E) Transient absorption spectra with the model alcohol substrate (**1o**) (40 mM) at 300 ns after laser excitation at 430 nm. (F) Transient absorption spectra with 4-methylanisole (40 mM) at 100 ns after laser excitation at 430 nm. (G) Transient absorption spectra with the model alcohol substrate (**1n**) (50 mM).

energy barrier compared with the stepwise PCET mechanism (pathway C). Consequently, the classical stepwise mechanism is thus the least kinetically favorable mechanism of the two (11.9 vs 9.4 kcal/mol). The non-PCET mechanism represents the most kinetically favorable path having the lowest barrier of 8.4 kcal/mol. Taking the accuracy of the DFT calculations into account, these results suggest that a non-PCET mechanism constitutes the main operating mechanism, but that a concerted PCET-based mechanism can operate in parallel. The initially postulated stepwise mechanism is most probably outcompeted by the fragmentative pathways. Taken together, these results indicate that the mechanistic features might be more complicated than what we previously thought.

To further our understanding of the mechanistic features, we conducted a series of steady-state and transient spectroscopy studies involving 4-methylanisole as a model substrate and three anisole derivatives harboring a primary, a secondary, and a tertiary benzylic alcohol (for experimental details see mechanistic study section in the ESI). The latter corresponds to substrate **1o**. Fluorescence quenching experiments revealed

https://doi.org/10.1021/acscatal.3c05150
ACS Catal. 2024, 14, 585−593

that the model substrate 4-methylanisole and all alcohol derivatives included in the study are good quenchers of the Fukuzumi catalyst (Figure 3C). While collidine itself partly quenched the fluorescence, the addition of collidine and substrate only showed an additive effect of the two quenchers, contrary to what we expected (Table S2 in ESI). This result supports that the substrate quenching is base-independent and that the excited state photocatalyst is quenched directly by the alcohol substrate and not by the hydrogen-bonded complex **1o-base**. The lack of a cooperative effect is perhaps not that startling considering the low concentration of such a complex in the reaction mixture ($K_{cal} \sim 0.002$ as estimated by the DFT calculations). Furthermore, these results indicate that the primary quenching can be ascribed to oxidation of the aromatic methoxybenzene unit rather than direct oxidation of the hydroxyl group since the model substrate 4-methylanisole is at least as good quencher as the alcohol derivatives.

Quenching of the fluorescence from the Fukuzumi catalyst was also measured as a function of the wavelength of the emitted light for 4-methylanisole and **1o** (Figure 3D). The fraction of quenching is clearly higher at lower wavelengths for 4-methylanisole as compared with **1o**, which has a peak quenching efficiency that is more red-shifted. The initial excited state of the Fukuzumi catalyst is an acridinium-localized singlet state that decays to an internal charge-transfer (CT) state, which has a red-shifted fluorescence with respect to that of the acridinium state.[28] The results show that anisole mostly quenches the initial acridinium state and that the alcohol substrate mostly quenches the CT state. Nanosecond transient absorption (ns-TA) experiments (see Figures S2−S4 in the ESI) showed that none of them quenches the Fukuzumi catalyst triplet excited state, which can be explained by the insufficient redox potential of the triplet state (E_{red} = +1.45 V vs SCE[28] which should be compared to E_{red} = +1.65 V vs SCE for *p*-methyl anisole[29]). The short lifetime of the singlet state (ca. 5 ps) necessitates a preassociation of the substrate with the catalyst, whereas the longer lifetime of the CT state (ca. 6 ns) can be quenched bimolecularly. Clearly, **1o** is less prone to complex formation with the Fukuzumi catalyst compared to 4-methylanisole. Differences in steric characteristics between the two substrates most probably explain these discrepancies. This observation suggests that to get excess to the higher oxidation potential of the acridinium singlet excited state of the Fukuzumi catalyst and its congeners, structural features that effect preassociation capability might be of importance generally in developing photocatalysis-based protocols.

Ns-TA experiments were performed to detect the transient photoproducts of the quenching reactions. The different excited and reduced states of the Fukuzumi catalyst exhibit strikingly similar spectra, with one key distinction: the triplet excited state has a clear peak at 565 nm, while the reduced acridine radical only has a tailing absorption.[28] By analyzing the absorbance ratio at 565/500 nm, we could therefore determine the abundance of triplets versus reduced radicals in the ns-TA spectrum. The ns-TA spectra of Fukuzumi catalyst with 4-methylanisole exhibit a notable shift toward the acridine radical (see a change in 565/500 nm ratio in Figure 3F), and with a positive contribution stemming from the methoxybenzene radical cation around 450 nm that counteracts the ground state bleach of the photocatalyst. The shift in the spectrum is instantaneous (we do not see the rise of the product on ns time scales), which strongly suggests that the product is generated from the singlet state or CT state. Notably, the addition of collidine does not affect the spectral change, as expected. This is true for all of the substrates investigated. Contrary to 4-methylanisole, the spectral features for all alcohol substrates shift from that of the triplet toward those of the acridine radical (see 565/500 nm ratio), but without the positive contribution from the methoxybenzene radical cation signal around 450 nm (Figure 3E, G). Taken together, this is strong (albeit indirect) evidence that intramolecular radical transfer happens in <20 ns for all the alcohol compounds and that the so-formed radical cationic species is converted to another species silent in the spectral range investigated in the same time frame. A reasonable conclusion is that the radical cation of 4-methylanisole persists on the ns time scale whereas the corresponding radical cations for the alcohol substrates rapidly convert to nonabsorbing species. The generation of both an oxygen-centered radical and a PCET-mediated or a non-PCET concerted fragmentation yielding the C-centered radical is consistent with these observations.

DFT calculations and spectroscopic investigations taken together support both a concerted PCET and a non-PCET mechanism. However, it is possible to draw a conclusion regarding which is the main operating mechanism. The rate constant for the non-PCET mechanism can be estimated rather accurately using the Eyring equation (calculated activation free energy $\Delta G‡$ = 8.4 kcal/mol, transmission coefficient κ = 1, temperature T = 293 K) to $k_{TS1} = 3.3 \times 10^6$ s^{-1}. It is also possible to rather accurately estimate the upper limit of the rate constant for the formation of the substrate base complex to be close to diffusion-controlled ($k_d = 7.7 \times 10^9$ dm^3 mol^{-1} s^{-1}). Furthermore, the concerted PCET is associated with a rate constant ($k_{TS2} = 3.0 \times 10^8$ s^{-1}) 2 orders of magnitude higher than that of both the non-PCET and the stepwise PCET ($k_{TS3} = 4.2 \times 10^6$ s^{-1}). The calculations thus suggest that the concerted PCET is highly favored over the stepwise PCET mechanism. However, due to that an endergonic pre-equilibrium needs to be established in the concerted PCET pathway B, the conditions employed favor the non-PCET pathway A as the major mechanism generating the targeted radical **IVa**. In fact, pathway A is predicted to be responsible for >90% of the generated radical **IVa** species (see the Supporting Information). This estimate holds true early in the reaction when assuming a fast equilibrium. The dominance of pathway A over pathway B will further increase as the reaction progresses as a consequence of a decreasing concertation of base, which will effect the equilibrium generating **II**. However, considering the steric nature of the substrate and the base, it is reasonable that the actual rate constant of the acid-base complex formation is much lower than the diffusion-controlled reaction rate constant. Taking the concentration of base and substrate together with the steric factors effecting the bimolecular reaction into account, direct fragmentation would be even more favored under conditions involving an equilibrium having a $k_1 < k_{TS1}$. An operating base-independent mechanism is also supported by the observation in a control experiment performed without base, which generated around 6% of the fragmentation-associated side product 4-methoxybenzaldehyde (Figure 4). Clearly, the base is necessary downstream of the deconstructive formation of the C-centered radical and also coupled to the turnover of the catalyst.

https://doi.org/10.1021/acscatal.3c05150
ACS Catal. 2024, 14, 585−593

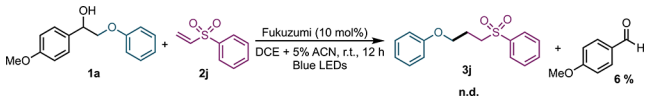

Figure 4. Control experiment performed without base.

Overall, the mechanistic study suggests that direct fragmentation (non-PCET) not only is an active pathway but also most probably the main mechanistic pathway. The non-PCET mechanism most likely operates in parallel with two PCET-based mechanisms, where a concerted fragmentation is suggested to be more favorable than the more commonly proposed mechanism involving an O-centered radical intermediate. To what extent these mechanisms compete in the reaction process is not yet clear. However, it is evident that the mechanistic features of these types of transformations are much more complex than what has previously been believed. In future investigations, we will continue to explore the mechanistic details of these reactions using femtosecond transient absorption spectroscopy.

CONCLUSIONS

In conclusion, an efficient metal-free photocatalytic method for the alkylation of alkenes by readily accessible acyclic aliphatic alcohols as redox auxiliaries has been developed. The mild conditions identified efficiently generated C-centered radicals, which have been employed in subsequent $C(sp^3)-C(sp^3)$ bond-forming processes. Overall, this method provides a C1 tethering strategy for nucleophiles and electrophiles. The optimized reaction conditions demonstrate a relatively broad substrate scope, accommodating various electron-deficient alkenes and a wide range of secondary and tertiary alcohols. Furthermore, the method was shown to be applicable in the late-stage functionalization of natural products and pharmaceutically relevant compounds.

The mechanistic investigations revealed that this specific deconstructive approach to C-centered radicals is more complex than it was previously thought. Multiple mechanisms, including non-PCET fragmentation and concerted/stepwise PCET, were identified through both experimental and computational studies. While the direct fragmentation pathway appeared to be active and potentially dominant, the PCET pathways most probably operated concurrently. These findings highlight the intricate and multifaceted nature of β-scission basted radical generation instigated via reductive quenching of photocatalysts. Further studies utilizing femtosecond transient absorption spectroscopy are necessary to unravel the intricate details of the mechanism. Together with such mechanistic studies, efforts are currently invested toward applications focusing on two- and three-component cross-coupling reactions involving aryl halides, alcohols, and alkenes.

ASSOCIATED CONTENT

Supporting Information

The Supporting Information is available free of charge at https://pubs.acs.org/doi/10.1021/acscatal.3c05150.

Experimental procedures and characterization data (PDF)

AUTHOR INFORMATION

Corresponding Author

Carl-Johan Wallentin − *Department of Chemistry and Molecular Biology, University of Gothenburg, Gothenburg SE 41296, Sweden;* orcid.org/0000-0003-1983-9378; Email: carl.wallentin@chem.gu.se

Authors

Yeersen Patehebieke − *Department of Chemistry and Molecular Biology, University of Gothenburg, Gothenburg SE 41296, Sweden*

Rima Charaf − *Department of Chemistry - Ångström Laboratories, Uppsala University, Uppsala SE 75120, Sweden*

Hogan P. Bryce-Rogers − *Department of Chemistry and Molecular Biology, University of Gothenburg, Gothenburg SE 41296, Sweden;* orcid.org/0000-0002-3186-9601

Ke Ye − *Department of Theoretical Chemistry & Biology, School of Engineering Sciences in Chemistry, Biotechnology and Health, KTH Royal Institute of Technology, Stockholm SE 10691, Sweden*

Mårten Ahlquist − *Department of Theoretical Chemistry & Biology, School of Engineering Sciences in Chemistry, Biotechnology and Health, KTH Royal Institute of Technology, Stockholm SE 10691, Sweden;* orcid.org/0000-0002-1553-4027

Leif Hammarström − *Department of Chemistry - Ångström Laboratories, Uppsala University, Uppsala SE 75120, Sweden;* orcid.org/0000-0002-9933-9084

Complete contact information is available at: https://pubs.acs.org/10.1021/acscatal.3c05150

Author Contributions

C. J. W. supervised the overall project. C. J. W. and Y. P. conceived the idea and designed the study with H. P. B. R. The synthesis, purification and characterizations are done by Y. P. and H. P. B. R. R. C. and L. H. contributed to the mechanistic study. K. Y. and M. A. contributed to the computational study. Y. P. and C. J. W. co-wrote the manuscript. All authors have given approval to the final version of the manuscript.

Funding

Financial support from the Knut and Alice Wallenberg Foundation (Grant 2019.0071) is gratefully acknowledged.

Notes

The authors declare no competing financial interest.

ACKNOWLEDGMENTS

A special recognition to Dr. Daniel Tietze (University of Gothenburg) for assistance with LC-(HR)MS.

REFERENCES

(1) (a) Chang, L.; An, Q.; Duan, L.; Feng, K.; Zuo, Z. Alkoxy Radicals See the Light: New Paradigms of Photochemical Synthesis. *Chem. Rev.* **2022**, *122* (2), 2429−2486. (b) Murray, P. R. D.; Cox, J. H.; Chiappini, N. D.; Roos, C. B.; McLoughlin, E. A.; Hejna, B. G.; Nguyen, S. T.; Ripberger, H. H.; Ganley, J. M.; Tsui, E.; Shin, N. Y.; Koronkiewicz, B.; Qiu, G.; Knowles, R. R. Photochemical and Electrochemical Applications of Proton-Coupled Electron Transfer in Organic Synthesis. *Chem. Rev.* **2022**, *122* (2), 2017−2291. (c) Morcillo, S. P. Radical-Promoted C−C Bond Cleavage: A Deconstructive Approach for Selective Functionalization. *Angew. Chem., Int. Ed.* **2019**, *58* (40), 14044−14054. (d) Yu, X.-Y.; Chen, J.-R.; Xiao, W.-J. Visible Light-Driven Radical-Mediated C−C Bond

Cleavage/Functionalization in Organic Synthesis. *Chem. Rev.* **2021**, *121* (1), 506−561. (e) Wu, X.; Zhu, C. Recent Advances in Alkoxy Radical-Promoted C−C and C−H Bond Functionalization Starting from Free Alcohols. *Chem. Commun.* **2019**, *55* (66), 9747−9756. (f) Jia, K.; Chen, Y. Visible-Light-Induced Alkoxyl Radical Generation for Inert Chemical Bond Cleavage/Functionalization. *Chem. Commun. (Cambridge, U. K.)* **2018**, *54* (48), 6105−6112.

(2) Tsui, E.; Wang, H.; Knowles, R. R. Catalytic Generation of Alkoxy Radicals from Unfunctionalized Alcohols. *Chem. Sci.* **2020**, *11* (41), 11124−11141.

(3) Tilvi, S.; Khan, S.; Majik, M. S. γ-Hydroxybutenolide Containing Marine Natural Products and Their Synthesis: A Review. *Curr. Org. Chem.* **2020**, *23* (22), 2436−2468.

(4) Diez-Torrubia, A.; Cabrera, S.; Lambeir, A.-M.; Balzarini, J.; Camarasa, M.-J.; Velázquez, S. Dipeptidyl Peptidase IV (DPPIV/CD26)-Based Prodrugs of Hydroxy-Containing Drugs. *ChemMedChem.* **2012**, *7* (4), 618−628.

(5) (a) Luk, H. T.; Mondelli, C.; Ferré, D. C.; Stewart, J. A.; Pérez-Ramírez, J. Status and Prospects in Higher Alcohols Synthesis from Syngas. *Chem. Soc. Rev.* **2017**, *46* (5), 1358−1426. (b) Goldemberg, J. Ethanol for a Sustainable Energy Future. *Science* **2007**, *315* (5813), 808−810.

(6) Roos, G.; Roos, C. Chapter 7 - Functional Classes II, Reactions. In *Organic Chemistry Concepts*; Roos, G.; Roos, C., Eds.; Academic Press, 2015; pp 103−149.

(7) Yang, J.-D.; Ji, P.; Xue, X.-S.; Cheng, J.-P. Recent Advances and Advisable Applications of Bond Energetics in Organic Chemistry. *J. Am. Chem. Soc.* **2018**, *140* (28), 8611−8623.

(8) (a) Barton, D. H. R.; Beaton, J. M.; Geller, L. E.; Pechet, M. M. A New Photochemical Reaction. *J. Am. Chem. Soc.* **1960**, *82* (10), 2640−2641. (b) Barton, D.; Beaton, J. A Synthesis of Aldosterone Acetate. *J. Am. Chem. Soc.* **1960**, *82* (10), 2641−2641.

(9) (a) Walling, C.; Clark, R. T. Reactions of Primary and Secondary Alkoxy Radicals Derived from Hypochlorites. *J. Am. Chem. Soc.* **1974**, *96* (14), 4530−4534. (b) Walling, C.; McGuinness, J. A. Positive Halogen Compounds. XVI. Comparison of Alkoxy Radicals from Different Sources and the Role of Halogen Atoms in Hypohalite Reactions. *J. Am. Chem. Soc.* **1969**, *91* (8), 2053−2058. (c) Heusler, K.; Kalvoda, J. Intramolecular Free-Radical Reactions. *Angew. Chem., Int. Ed. Engl.* **1964**, *3* (8), 525−538.

(10) (a) Guan, H.; Sun, S.; Mao, Y.; Chen, L.; Lu, R.; Huang, J.; Liu, L. Iron (II)-Catalyzed Site-Selective Functionalization of Unactivated C (sp^3)−H Bonds Guided by Alkoxyl Radicals. *Angew. Chem.* **2018**, *130* (35), 11583−11587. (b) DiRocco, D. A.; Dykstra, K.; Krska, S.; Vachal, P.; Conway, D. V.; Tudge, M. Late-Stage Functionalization of Biologically Active Heterocycles Through Photoredox Catalysis. *Angew. Chem., Int. Ed.* **2014**, *53* (19), 4802−4806. (c) Čeković, Z. I.; Cvetković, M. Functionallization of the δ-Carbon Atom by the Ferrous Ion Induced Decomposition of Alkyl Hydroperoxides in the Presence of Cupric Salts. *Tetrahedron Lett.* **1982**, *23* (37), 3791−3794. (d) Kochi, J. K. Chemistry of Alkoxy Radicals: Cleavage Reactions. *J. Am. Chem. Soc.* **1962**, *84* (7), 1193−1197.

(11) (a) Pasto, D. J.; Cottard, F. Demonstration of the Synthetic Utility of the Generation of Alkoxy Radicals by the Photo-Induced Homolytic Dissociation of Alkyl 4-nitrobenzenesulfenates. *Tetrahedron Lett.* **1994**, *35* (25), 4303−4306. (b) Beckwith, A. L.; Hay, B. P.; Williams, G. M. Generation of Alkoxyl Radicals from O-alkyl Benzenesulphenates. *J. Chem. Soc., Chem. Commun.* **1989**, *17*, 1202−1203.

(12) (a) Zhang, J.; Li, Y.; Xu, R.; Chen, Y. Donor−Acceptor Complex Enables Alkoxyl Radical Generation for Metal-Free C(sp^3)−C(sp^3) Cleavage and Allylation/Alkenylation. *Angew. Chem.* **2017**, *129* (41), 12793−12797. (b) Zhang, J.; Li, Y.; Zhang, F.; Hu, C.; Chen, Y. Generation of Alkoxyl Radicals by Photoredox Catalysis Enables Selective C(sp^3)−H Functionalization Under Mild Reaction Conditions. *Angew. Chem., Int. Ed.* **2016**, *55* (5), 1872−1875. (c) Cong, F.; Lv, X.-Y.; Day, C. S.; Martin, R. Dual Catalytic Strategy for Forging sp^2−sp^3 and sp^3−sp^3 Architectures via β-Scission of Aliphatic Alcohol Derivatives. *J. Am. Chem. Soc.* **2020**, *142* (49), 20594−20599.

(13) (a) Bao, X.; Wang, Q.; Zhu, J. Dual Photoredox/Copper Catalysis for the Remote C (sp^3)−H Functionalization of Alcohols and Alkyl Halides by N-Alkoxypyridinium Salts. *Angew. Chem., Int. Ed.* **2019**, *58* (7), 2139−2143. (b) Kim, I.; Park, B.; Kang, G.; Kim, J.; Jung, H.; Lee, H.; Baik, M. H.; Hong, S. Visible-Light-Induced Pyridylation of Remote C(sp^3)−H Bonds by Radical Translocation of N-Alkoxypyridinium Salts. *Angew. Chem., Int. Ed.* **2018**, *57* (47), 15517−15522. (c) Barthelemy, A. L.; Tuccio, B.; Magnier, E.; Dagousset, G. Alkoxyl Radicals Generated under Photoredox Catalysis: A Strategy for anti-Markovnikov Alkoxylation Reactions. *Angew. Chem., Int. Ed.* **2018**, *57* (42), 13790−13794.

(14) Kim, S.; Lee, T. A.; Song, Y. Facile Generation of Alkoxy Radicals from N-alkoxyphthalimides. *Synlett* **1998**, *1998* (05), 471−472.

(15) (a) Leffler, J. E. Cleavages and Rearrangements Involving Oxygen Radicals and Cations. *Chem. Rev.* **1949**, *45* (3), 385−417. (b) Chattaway, F. D.; Backeberg, O. G. CCCLVI.—Alkyl hypochlorites. *J. Chem. Soc., Trans.* **1923**, *123*, 2999−3003. (c) Beckwith, A. L.; Hay, B. P. Generation of Alkoxy Radicals from N-alkoxypyridinethiones. *J. Am. Chem. Soc.* **1988**, *110* (13), 4415−4416.

(16) Barton, D. H. R.; Beaton, J. M. A Synthesis of Aldosterone Acetate. *J. Am. Chem. Soc.* **1960**, *82* (10), 2641−2641.

(17) (a) Zhao, H.; Fan, X.; Yu, J.; Zhu, C. Silver-Catalyzed Ring-Opening Strategy for the Synthesis of β-and γ-Fluorinated Ketones. *J. Am. Chem. Soc.* **2015**, *137* (10), 3490−3493. (b) Ren, R.; Zhao, H.; Huan, L.; Zhu, C. Manganese-Catalyzed Oxidative Azidation of Cyclobutanols: Regiospecific Synthesis of Alkyl Azides by C−C Bond Cleavage. *Angew. Chem., Int. Ed.* **2015**, *54* (43), 12692−12696. (c) Ren, R.; Wu, Z.; Xu, Y.; Zhu, C. C−C Bond-Forming Strategy by Manganese-Catalyzed Oxidative Ring-Opening Cyanation and Ethynylation of Cyclobutanol Derivatives. *Angew. Chem., Int. Ed.* **2016**, *55* (8), 2866−2869. (d) Zhu, Y.; Zhang, Z.; Jin, R.; Liu, J.; Liu, G.; Han, B.; Jiao, N. DMSO-Enabled Selective Radical O−H Activation of 1, 3 (4)-Diols. *Angew. Chem.* **2020**, *132* (45), 20023−20028. (e) Li, G.-X.; Hu, X.; He, G.; Chen, G. Photoredox-Mediated Remote C(sp^3)−H Heteroarylation of Free Alcohols. *Chem. Sci.* **2019**, *10* (3), 688−693. (f) Jia, K.; Zhang, F.; Huang, H.; Chen, Y. Visible-Light-Induced Alkoxyl Radical Generation Enables Selective C(sp^3)−C(sp^3) Bond Cleavage and Functionalizations. *J. Am. Chem. Soc.* **2016**, *138* (5), 1514−1517. (g) Wu, X.; Wang, M.; Huan, L.; Wang, D.; Wang, J.; Zhu, C. Tertiary-Alcohol-Directed Functionalization of Remote C(sp^3)−H Bonds by Sequential Hydrogen Atom and Heteroaryl Migrations. *Angew. Chem., Int. Ed.* **2018**, *57* (6), 1640−1644. (h) Jia, K.; Pan, Y.; Chen, Y. Selective Carbonyl−C(sp^3) Bond Cleavage to Construct Ynamides, Ynoates, and Ynones by Photoredox Catalysis. *Angew. Chem.* **2017**, *129* (9), 2518−2521. (i) Zhu, Y.; Huang, K.; Pan, J.; Qiu, X.; Luo, X.; Qin, Q.; Wei, J.; Wen, X.; Zhang, L.; Jiao, N. Silver-Catalyzed Remote Csp^3−H Functionalization of Aliphatic Alcohols. *Nat. Commun.* **2018**, *9* (1), 2625. (j) Rivero, A. R.; Fodran, P.; Ondrejková, A.; Wallentin, C.-J. Alcohol Etherification via Alkoxy Radicals Generated by Visible-Light Photoredox Catalysis. *Org. Lett.* **2020**, *22* (21), 8436−8440.

(18) Guo, J. J.; Hu, A.; Chen, Y.; Sun, J.; Tang, H.; Zuo, Z. Photocatalytic C−C Bond Cleavage and Amination of Cycloalkanols by Cerium (III) Chloride Complex. *Angew. Chem., Int. Ed.* **2016**, *55* (49), 15319−15322.

(19) Yayla, H. G.; Wang, H.; Tarantino, K. T.; Orbe, H. S.; Knowles, R. R. Catalytic Ring-Opening of Cyclic Alcohols Enabled by PCET Activation of Strong O−H Bonds. *J. Am. Chem. Soc.* **2016**, *138* (34), 10794−10797.

(20) (a) Zhao, K.; Yamashita, K.; Carpenter, J. E.; Sherwood, T. C.; Ewing, W. R.; Cheng, P. T.; Knowles, R. R. Catalytic Ring Expansions of Cyclic Alcohols Enabled by Proton-Coupled Electron Transfer. *J. Am. Chem. Soc.* **2019**, *141* (22), 8752−8757. (b) Zhao, K.; Seidler, G.; Knowles, R. R. 1, 3-Alkyl Transposition in Allylic Alcohols Enabled by Proton-Coupled Electron Transfer. *Angew. Chem., Int. Ed.* **2021**, *60* (37), 20190−20195. (c) Nguyen, S. T.; McLoughlin, E. A.;

https://doi.org/10.1021/acscatal.3c05150
ACS Catal. 2024, 14, 585−593

Cox, J. H.; Fors, B. P.; Knowles, R. R. Depolymerization of Hydroxylated Polymers via Light-Driven C−C Bond Cleavage. *J. Am. Chem. Soc.* **2021**, *143* (31), 12268−12277. (d) Tsui, E.; Metrano, A. J.; Tsuchiya, Y.; Knowles, R. R. Catalytic Hydroetherification of Unactivated Alkenes Enabled by Proton-Coupled Electron Transfer. *Angew. Chem., Int. Ed.* **2020**, *59* (29), 11845−11849. (e) Ota, E.; Wang, H.; Frye, N. L.; Knowles, R. R. A Redox Strategy for Light-Driven, Out-of-Equilibrium Isomerizations and Application to Catalytic C−C Bond Cleavage Reactions. *J. Am. Chem. Soc.* **2019**, *141* (4), 1457−1462. (f) Hu, A.; Guo, J.-J.; Pan, H.; Tang, H.; Gao, Z.; Zuo, Z. δ-Selective Functionalization of Alkanols Enabled by Visible-Light-Induced Ligand-to-Metal Charge Transfer. *J. Am. Chem. Soc.* **2018**, *140* (5), 1612−1616. (g) Hu, A.; Guo, J.-J.; Pan, H.; Zuo, Z. Selective Functionalization of Methane, Ethane, and Higher Alkanes by Cerium Photocatalysis. *Science* **2018**, *361* (6403), 668−672. (h) Du, J.; Yang, X.; Wang, X.; An, Q.; He, X.; Pan, H.; Zuo, Z. Photocatalytic Aerobic Oxidative Ring Expansion of Cyclic Ketones to Macrolactones by Cerium and Cyanoanthracene Catalysis. *Angew. Chem., Int. Ed.* **2021**, *60* (10), 5370−5376. (i) An, Q.; Wang, Z.; Chen, Y.; Wang, X.; Zhang, K.; Pan, H.; Liu, W.; Zuo, Z. Cerium-catalyzed C−H Functionalizations of Alkanes Utilizing Alcohols as Hydrogen Atom Transfer Agents. *J. Am. Chem. Soc.* **2020**, *142* (13), 6216−6226. (j) Zhang, K.; Chang, L.; An, Q.; Wang, X.; Zuo, Z. Dehydroxymethylation of Alcohols Enabled by Cerium Photocatalysis. *J. Am. Chem. Soc.* **2019**, *141* (26), 10556−10564. (k) Hu, A.; Chen, Y.; Guo, J.-J.; Yu, N.; An, Q.; Zuo, Z. Cerium-Catalyzed Formal Cycloaddition of Cycloalkanols with Alkenes through Dual Photoexcitation. *J. Am. Chem. Soc.* **2018**, *140* (42), 13580−13585.

(21) (a) Huang, L.; Ji, T.; Rueping, M. Remote Nickel-Catalyzed Cross-Coupling Arylation via Proton-Coupled Electron Transfer-Enabled C−C Bond Cleavage. *J. Am. Chem. Soc.* **2020**, *142* (7), 3532−3539. (b) Wang, Y.; He, J.; Zhang, Y. $CeCl_3$-Promoted Simultaneous Photocatalytic Cleavage and Amination of Cα−Cβ Bond in Lignin Model Compounds and Native Lignin. *CCS Chemistry* **2020**, *2* (3), 107−117. (c) Huang, L.; Ji, T.; Zhu, C.; Yue, H.; Zhumabay, N.; Rueping, M. Bioinspired Desaturation of Alcohols Enabled by Photoredox Proton-Coupled Electron Transfer and Cobalt Dual Catalysis. *Nat. Commun.* **2022**, *13* (1), 809. (d) Ji, T.; Chen, X.-Y.; Huang, L.; Rueping, M. Remote Trifluoromethylthiolation Enabled by Organophotocatalytic C−C Bond Cleavage. *Org. Lett.* **2020**, *22* (7), 2579−2583. (e) Kikuchi, T.; Yamada, K.; Yasui, T.; Yamamoto, Y. Synthesis of Benzo-Fused Cyclic Ketones via Metal-Free Ring Expansion of Cyclopropanols Enabled by Proton-Coupled Electron Transfer. *Org. Lett.* **2021**, *23* (12), 4710−4714. (f) Varabyeva, N.; Barysevich, M.; Aniskevich, Y.; Hurski, A. $Ti(OiPr)_4$-Enabled Dual Photoredox and Nickel-Catalyzed Arylation and Alkenylation of Cyclopropanols. *Org. Lett.* **2021**, *23* (14), 5452−5456. (g) Zhao, T.-T.; Yu, W.-L.; Feng, Z.-T.; Qin, H.-N.; Zheng, H.-X.; Xu, P.-F. Photoredox/Nickel Dual Catalyzed Stereospecific Synthesis of Distal Alkenyl Ketones. *Chem. Commun.* **2022**, *58* (8), 1171−1174. (h) Wang, X.; Li, Y.; Wu, X. Photoredox/Cobalt Dual Catalysis Enabled Regiospecific Synthesis of Distally Unsaturated Ketones with Hydrogen Evolution. *ACS Catal.* **2022**, *12* (6), 3710−3718. (i) Yang, Z.; Yang, D.; Zhang, J.; Tan, C.; Li, J.; Wang, S.; Zhang, H.; Huang, Z.; Lei, A. Electrophotochemical Ce-Catalyzed Ring-Opening Functionalization of Cycloalkanols under Redox-Neutral Conditions: Scope and Mechanism. *J. Am. Chem. Soc.* **2022**, *144* (30), 13895−13902. (j) Liu, W.; Wu, Q.; Wang, M.; Huang, Y.; Hu, P. Iron-Catalyzed C−C Single-Bond Cleavage of Alcohols. *Org. Lett.* **2021**, *23* (21), 8413−8418. (k) Wu, Q.; Liu, W.; Wang, M.; Huang, Y.; Hu, P. Iron-Catalyzed Deconstructive Alkylation Through Chlorine Radical Induced C−C Single Bond Cleavage Under Visible Light. *Chem. Commun.* **2022**, *58* (71), 9886−9889. (l) Xue, T.; Zhang, Z.; Zeng, R. Photoinduced Ligand-to-Metal Charge Transfer (LMCT) of Fe Alkoxide Enabled C−C Bond Cleavage and Amination of Unstrained Cyclic Alcohols. *Org. Lett.* **2022**, *24* (3), 977−982.

(22) Zhao, K.; Yamashita, K.; Carpenter, J. E.; Sherwood, T. C.; Ewing, W. R.; Cheng, P. T. W.; Knowles, R. R. Catalytic Ring Expansions of Cyclic Alcohols Enabled by Proton-Coupled Electron Transfer. *J. Am. Chem. Soc.* **2019**, *141* (22), 8752−8757.

(23) (a) Salaverri, N.; Carli, B.; Gratal, P. B.; Marzo, L.; Alemán, J. Remote Giese Radical Addition by Photocatalytic Ring Opening of Activated Cycloalkanols. *Adv. Synth. Catal.* **2022**, *364* (10), 1689−1694. (b) Liao, K.; Wu, F.; Chen, J.; Huang, Y. Catalytic Cleavage and Functionalization of Bulky and Inert Csp^3−Csp^3 Bonds via A Relayed Proton-Coupled Electron Transfer Strategy. *Cell Reports Physical Science* **2022**, *3* (2), No. 100763.

(24) For more details, see Supporting Information.

(25) (a) Xiong, Y.; Zhang, X.; Guo, H.-M.; Wu, X. Photoredox/Persistent Radical Cation Dual Catalysis for Alkoxy Radical Generation from Alcohols. *Org. Chem. Front.* **2022**, *9* (13), 3532−3539. (b) Shu, W.; Zhang, H.; Huang, Y. γ-Alkylation of Alcohols Enabled by Visible-Light Induced 1,6-Hydrogen Atom Transfer. *Org. Lett.* **2019**, *21* (15), 6107−6111. (c) Xue, F.; Wang, F.; Liu, J.; Di, J.; Liao, Q.; Lu, H.; Zhu, M.; He, L.; He, H.; Zhang, D.; Song, H.; Liu, X. Y.; Qin, Y. A Desulfurative Strategy for the Generation of Alkyl Radicals Enabled by Visible-Light Photoredox Catalysis. *Angew. Chem.* **2018**, *130* (22), 6777−6781. (d) Zhou, R.; Goh, Y. Y.; Liu, H.; Tao, H.; Li, L.; Wu, J. Visible-Light-Mediated Metal-Free Hydrosilylation of Alkenes through Selective Hydrogen Atom Transfer for Si−H Activation. *Angew. Chem.* **2017**, *129* (52), 16848−16852.

(26) (a) Baciocchi, E.; Bietti, M.; Gerini, M. F.; Manduchi, L.; Salamone, M.; Steenken, S. Structural Effects on the OH^--Promoted Fragmentation of Methoxy-Substituted 1-Arylalkanol Radical Cations in Aqueous Solution: The Role of Oxygen Acidity. *Chem.—Eur. J.* **2001**, *7* (7), 1408−1416. (b) Baciocchi, E.; Bietti, M.; Lanzalunga, O. Mechanistic Aspects of β-Bond-Cleavage Reactions of Aromatic Radical Cations. *Acc. Chem. Res.* **2000**, *33* (4), 243−251.

(27) (a) Romero, N. A.; Margrey, K. A.; Tay, N. E.; Nicewicz, D. A. Site-selective arene C-H amination via photoredox catalysis. *Science* **2015**, *349* (6254), 1326−1330. (b) Tay, N. E. S.; Nicewicz, D. A. Cation Radical Accelerated Nucleophilic Aromatic Substitution via Organic Photoredox Catalysis. *J. Am. Chem. Soc.* **2017**, *139* (45), 16100−16104. (c) Margrey, K. A.; Levens, A.; Nicewicz, D. A. Direct Aryl C−H Amination with Primary Amines Using Organic Photoredox Catalysis. *Angew. Chem., Int. Ed.* **2017**, *56* (49), 15644−15648. (d) Margrey, K. A.; McManus, J. B.; Bonazzi, S.; Zecri, F.; Nicewicz, D. A. Predictive Model for Site-Selective Aryl and Heteroaryl C−H Functionalization via Organic Photoredox Catalysis. *J. Am. Chem. Soc.* **2017**, *139* (32), 11288−11299.

(28) Benniston, A. C.; Harriman, A.; Li, P.; Rostron, J. P.; van Ramesdonk, H. J.; Groeneveld, M. M.; Zhang, H.; Verhoeven, J. W. Charge shift and triplet state formation in the 9-mesityl-10-methylacridinium cation. *J. Am. Chem. Soc.* **2005**, *127* (46), 16054−16064.

(29) Roth, H. G.; Romero, N. A.; Nicewicz, D. A. Experimental and Calculated Electrochemical Potentials of Common Organic Molecules for Applications to Single-Electron Redox Chemistry. *Synlett* **2016**, *27* (05), 714−723.

https://doi.org/10.1021/acscatal.3c05150
ACS Catal. 2024, 14, 585−593